Received: 9 October 2017 | Revised: 2 November 2017 | Accepted: 2 November 2017

DOI: 10.1002/aoc.4200

FULL PAPER

WILEY Applied Organometallic Chemistry

(Benzyl isocyanide)gold(I) pyrimidine-2-thiolate complex: Synthesis and biological activity

Masood Fereidoonnezhad[1] | Hamid R. Shahsavari[2] | Elaheh Lotfi[1] | Mojgan Babaghasabha[2] | Motahareh Fakhri[1] | Zeinab Faghih[3] | Zahra Faghih[4] | M. Hassan Beyzavi[5]

[1] Department of Medicinal Chemistry, School of Pharmacy, and Cancer, Environmental and Petroleum Pollutants Research Center, Ahvaz Jundishapur University of Medical Sciences, Ahvaz, Iran

[2] Department of Chemistry, Institute for Advanced Studies in Basic Sciences (IASBS), Yousef Sobouti Blvd, Zanjan 45137-66731, Iran

[3] Pharmaceutical Sciences Research Center, Shiraz University of Medical Sciences, Shiraz, Iran

[4] Shiraz Institute for Cancer Research, School of Medicine, Shiraz University of Medical Sciences, Shiraz, Iran

[5] Department of Chemistry and Biochemistry, University of Arkansas, Fayetteville, AR 72701, U.S.A.

Correspondence
Hamid R. Shahsavari, Department of Chemistry, Institute for Advanced Studies in Basic Sciences (IASBS), Yousef Sobouti Blvd, Zanjan 45137-66731, Iran.
Email: shahsavari@iasbs.ac.ir

M. Hassan Beyzavi, Department of Chemistry and Biochemistry, University of Arkansas, Fayetteville, AR 72701, U.S.A.
Email: beyzavi@uark.edu

Funding information
University of Arkansas, Institute for Advanced Studies in Basic Sciences (IASBS) Research Council and Ahvaz Jundishapur University of Medical Sciences.

The reaction of [(Me_2S)AuCl] with an equimolar amount of benzyl isocyanide ($PhCH_2NC$) ligand led to the formation of complex [($PhCH_2NC$)AuCl] (**1**). The solid-state structure of **1** was determined using the X-ray diffraction method. Through a salt metathesis reaction, the chloride ligand in **1** was replaced by pyrimidine-2-thiolate ($SpyN^-$) to afford the complex [($PhCH_2NC$)Au(η^1-S-Spy)] (**2**), which was characterized spectroscopically. The cytotoxic activities of **1** and **2** were evaluated against three human cancer cell lines: ovarian carcinoma (SKOV3), lung carcinoma (A549) and breast carcinoma (MCF-7). Complex **2** showed higher cytotoxicity than cisplatin against SKOV3 and MCF-7 cancer cell lines. It showed a strong anti-proliferative activity with IC_{50} of 7.80, 6.26 and 6.14 μM, compared with that measured for cisplatin which was 7.62, 12.36 and 11.47 μM, against A549, SKOV3 and MCF-7 cell lines, respectively. The induction of cellular apoptosis by **2** was also studied on MCF-7 cell line. Our results indicated that **2** could induce apoptosis in cancerous cells in a dose-dependent manner.

KEYWORDS
apoptosis study, biological activity, gold complexes, isocyanide ligand, thiolate ligand

1 | INTRODUCTION

Since the discovery of cisplatin in the mid-1960s,[1] there has been a growing attention towards Pt-based anti-proliferative drugs. However, the Pt-based treatment of cancer is significantly impeded by the development of resistance and severe side-effects. Sulfur-containing biomolecules play a pivotal role in Pt anti-proliferative chemotherapy because of their high affinity to the Pt(II) ion.[2,3] Irreversible and strong binding of cisplatin to intracellular thiolato donors is hypothesized to be an important cause of inactivation. As a result, novel metal-based anti-tumour complexes with pharmacological characteristics other than Pt-based drugs are an important target in modern drug design and medicinal chemistry. In recent years, Au-based complexes have received increasing consideration because of their potent inhibition of cancer cell growth which is mainly caused by non-cisplatin-like mechanisms of action.[4]

Gold is an important transition metal that has two significant oxidation states, +1 and +3.[5] It is believed that the most stable oxidation state of Au is Au(I) and it forms usual linear complexes by coordination of two ligands.[6] The stability of Au(I) complexes is straightforwardly modified by the nature of the coordinating ligands, i.e. donor atoms.[7–10] These complexes usually comprise soft donor atoms such as carbon,[11–17] phosphorus[18–21] and sulfur.[21–24]

Organic compounds containing a thiol group (RSH) or its corresponding anion form, called thiolate (RS^-), are chemically unique and can be used as a source of sulfur donor ligands.[3,25–27] Several complexes based on thiolate ligands especially of the type L–Au(I)–SR have been prepared. In these complexes L is a neutral ligand such as phosphine,[24,28–30] N-heterocyclic carbene[31–33] or isocyanide.[28,34–36] In general, the presence of the various L donor ligands and thiolate ligands in the structure of these complexes leads to a wide range of applications particularly in cancer treatment.[24,29,31,33]

The present paper demonstrates the synthesis, structural characterization and biological activity of new Au(I) complexes with isocyanide and thiolate ligands. The biological activity was evaluated on three different cancer cell lines. In addition, the study included an investigation of the capacity of these compounds to induce apoptosis.

2 | RESULTS AND DISCUSSION

2.1 | Synthesis and characterization of complexes

The precursor complex [(Me_2S)AuCl] (**A**) was prepared according to the report of Puddephatt and co-workers.[37] The SMe_2 ligand in **A** is a good leaving group and can be readily substituted by one equivalent of benzyl isocyanide ($PhCH_2NC$) which afforded the corresponding complex [($PhCH_2NC$)AuCl] (**1**).[38] Hashmi and co-workers[13,38] have also reported **1**, but utilizing a different precursor complex: [(tht)AuCl] (tht = tetrahydrothiophene). We further treated **1** with potassium pyrimidine-2-thiolate (KSpyN) in a 1:1 molar ratio which yielded complex [($PhCH_2NC$)Au(η^1-S-Spy)] (**2**) as a new complex through a salt metathesis reaction (Scheme 1). Both complexes are air-stable, colourless solids that were obtained in good yields. Complexes **1** and **2** were characterized using NMR and infrared (IR) spectroscopy and elemental analysis, and the solid-state structure of **1** was further confirmed for the first time using single-crystal X-ray diffraction.

IR spectra of **1** and **2** (in KBr) exhibited distinctive bands at 2260 and 2247 cm^{-1}, respectively, which are related to the stretching frequency of isocyanide function. The observed bands had a hypsochromic shift with respect to that of the $PhCH_2NC$ free ligand (2149 cm^{-1})[39,40] and they supported standard coordination (direct end-on mode) of the isocyanide function to the Au atom in both complexes.[28,35]

The ^1H NMR and $^{13}C\{^1H\}$ NMR spectra of **1** and **2** (in $CDCl_3$) displayed signal resonances due to the $PhCH_2NC$ ligand in expected regions (similar to the free ligand,[39,40] with slight shifts) and a simple pattern for the SpyN ligand in **2** (Figures S1 and S2). Also, in the $^{13}C\{^1H\}$ NMR spectra of both complexes, C^e and C^f of $PhCH_2NC$ ligand indicated a resolving coupling with nitrogen nucleus (^{14}N) which is a characteristic feature for numerous isocyanide ligands and their complexes (Figures S1 and S2).[12,13]

Single-crystal X-ray diffraction was carried out using **1** to determine its molecular structure, and crystallographic data are collected in Table S1. Appropriate crystals of **1** were obtained from its CH_2Cl_2 solution with slow layer diffusion of *n*-hexane. This complex crystallizes in the monoclinic crystal system (space group $P2_1/c$). The ORTEP view of **1** is shown in Figure 1 and selected bond lengths and angles are provided in the caption. Complex **1** has a quasilinear C2–N1–C1–Au–Cl1 skeleton extending from the centre of benzylic carbon atom of the isocyanide ligand to the chloride atom. The C1—Au—Cl1 (177.7(4)°) and C1—N1—C2 (176.8(14)°) angles are close to 180°. The Au—C1 and Au—Cl1 bond distances are close to the values observed for (isocyanide)Au(I) halide complexes like [(PhNC)AuCl].[12] In the lattice of this structure all molecular units are crystallographically equivalent and the molecules are aggregated to form an infinite zigzag chain[12,41] with a sequence of the monomers in an antiparallel arrangement (Figure S3). Additionally, a network of hydrogen bonds arises between

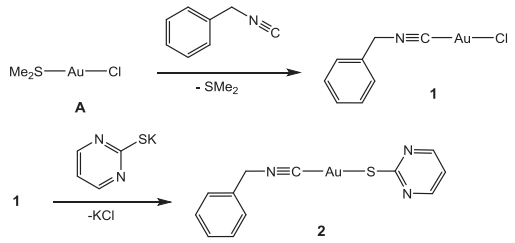

SCHEME 1 Synthetic routes for preparation of **1** and **2**

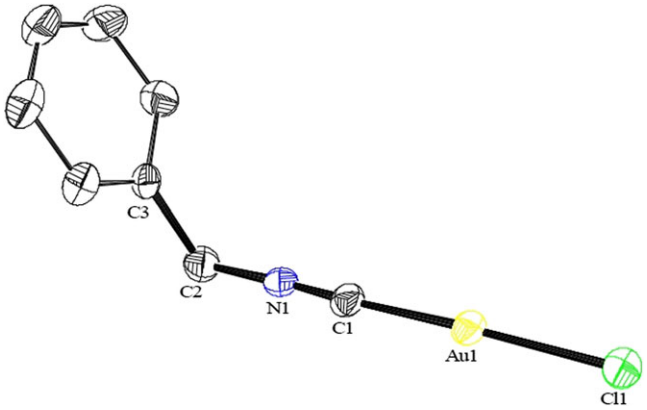

FIGURE 1 Representation of X-ray crystal of **1** showing all non-hydrogen atoms as 40% thermal ellipsoids. Selected geometric parameters: bond lengths (Å) Au1–C1, 1.932(16); Au1–Cl1, 2.263(4); N1–C1, 1.129(17); N1–C2, 1.43(2); bond angles (°) C1–Au1–Cl1, 177.7(4); Au1–C1–N1, 177.6(12); C1–N1–C2, 176.8(14); N1–C2–C3, 111.1(14)

hydrogen atoms of benzylic carbons and chloride ligands (Figure S3). In this supramolecular arrangement, no aurophilic interactions are observed between neighbour Au atoms (Au–Au distances are 4.519–4.570 Å). This observation may be related to the close antiparallel packing in layers, forcing the Au atoms into alternating positions above and below the plane.[12,41]

2.2 | Biological activity

The *in vitro* cytotoxicity effects of **1** and **2** were evaluated on three cancer cell lines: ovarian carcinoma (SKOV3), lung carcinoma (A549) and breast carcinoma (MCF-7). As evident from Table 1, the most active compound of this series, **2**, exhibited greater cytotoxicity than cisplatin against SKOV3 and MCF-7 cancer cell lines. However, its cytotoxicity against the A549 cell line was comparable with that of cisplatin. It showed a strong anti-proliferative activity with IC_{50} of 7.80, 6.26 and 6.14 μM, compared with that measured for cisplatin which was 7.62, 12.36 and 11.47 μM, against A549, SKOV3 and MCF-7 cell lines, respectively. Complex **1** also showed a moderate anti-tumour effect, comparable with that of cisplatin, especially against MCF-7 cell line with IC_{50} of 10.15 μM (Figure 2). According to these results, the factors affecting the activity of the synthesized Au(I) complexes can be obtained and the relationship between structure and activity could be acquired. Based on the structure, it can be concluded that the presence of thiolate ligand (pyrimidine-2-thiolate in **2**) increases the cytotoxicity. The presence of chloro group instead of thiolate ligand decreases the anti-proliferative activity. Also, **2** displays higher cytotoxicity against MCF-7 cell line than similar complexes such as phosphine-bridged dinuclear Au(I) alkynyl,[42] Au(I)–alkynyl chromones[43] and Au(I)–carbene complexes.[44]

TABLE 1 *In vitro* cytotoxic activity of gold complexes against cancer cell lines

	IC_{50} ± SD (μM)		
Complex	**A549**	**SKOV3**	**MCF-7**
1	22.66 ± 3.76	22.25 ± 3.56	10.15 ± 1.15
2	7.80 ± 0.64	6.26 ± 0.72	6.14 ± 0.41
Cisplatin	7.62 ± 0.68	12.36 ± 1.07	11.47 ± 1.29

2.3 | Apoptotic effect of 2 on MCF-7 cell line

Apoptosis, or programmed cell death, is a normal process that plays an important role in maintaining tissue homeostasis during embryonic development as well as pathological conditions through removal of unwanted or damaged cells. In the present study we used BioLegend's FITC Annexin V Apoptosis Detection Kit with PI (BioLegend, USA) to specifically identify apoptotic and necrotic cells during treatment by **2**. Annexin V is one of the intracellular proteins that can bind to phosphatidylserine (PS) which is normally found on the intracellular leaflet of the plasma membrane in live cells. During early apoptosis, as a result of losing membrane asymmetry, PS translocates to the external leaflet and therefore can be specifically targeted by fluorochrome-labelled Annexin V. Translocation of PS is followed by the loss of membrane integrity. Therefore, we also simultaneously used 7-aminoactinomycin D (7-AAD) to distinguish between necrotic and apoptotic cells. 7-AAD is a DNA binding reagent with a high constant which is efficiently excluded by live healthy as well as early apoptotic cells, but penetrates into the nucleus of damaged cells, i.e. late-stage apoptotic cells and necrotic cells, and stains the DNA. To determine the dose-dependent effect of **2**, the three dilutions of this compound with 2.5, 5 and 10 μM concentrations were prepared and the apoptotic effects was assessed on MCF-7 cell line. As can be seen in Figure 3, the percentage of cells in early apoptotic phase markedly increased from 4.55% in untreated cells to 15.70, 64.40 and 71.60% in cells treated with 2.5, 5 and 10 μM of **2**,

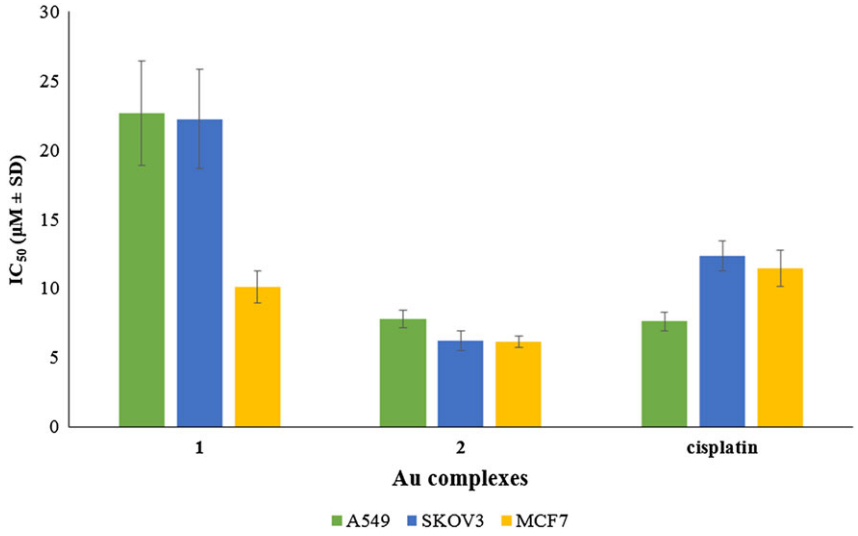

FIGURE 2 IC_{50} values of **1** and **2** against A549, SKOV3 and MCF-7 cancer cell lines

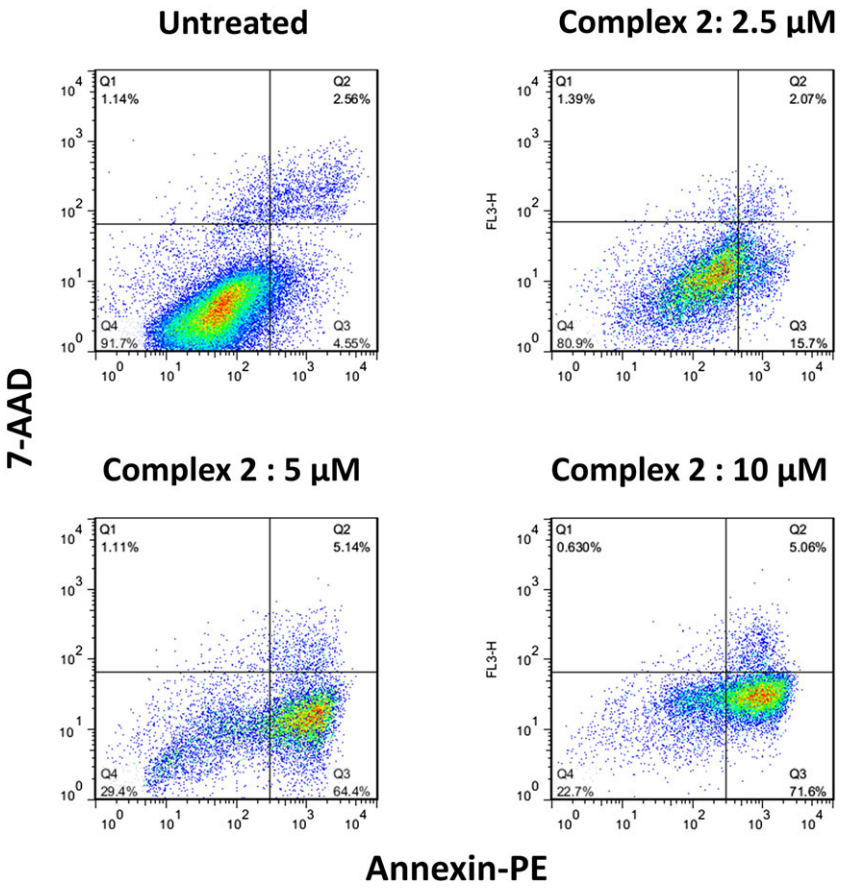

FIGURE 3 Anti-apoptotic effect of **2** on MCF-7 cell line. Compared to untreated cells, the percentage of MCF-7 cells in early apoptotic phase (7AAD−/Annexin V+) markedly increased in the cells treated with 2.5, 5 and 10 μM of **2** in a dose-dependent manner. 7AAD stains dead cells. 7AAD−/Annexin V+: early apoptosis; 7AAD+/Annexin V+: late apoptosis; 7AAD+/Annexin V−: necrosis; 7AAD−/Annexin V−: viable cells

respectively. These results show that this compound can induce apoptosis in cancerous cells in a dose-dependent manner.

3 | CONCLUSIONS

Due to the limitations of cisplatin, Au complexes have received considerable attention for their anti-tumour activities. While phosphine and nitrogen donors are well explored, herein, a new sulfur-based Au complex, **2**, is reported. The linear d^{10} two-coordinate complex **1** is readily prepared in high yield by replacement of dimethylsulfide ligand in **A** with benzyl isocyanide. NMR spectroscopy and X-ray diffraction confirmed the structure of **1**. The chemistry of **1** was explored in a salt metathesis reaction. In this reaction an anion exchange between **1** and potassium pyrimidine-2-thiolate occurs

leading to the formation of **2**. Its structure was characterized using NMR spectroscopy. The cytotoxic activities of **1** and **2** were screened against various cancer cell lines. The *in vitro* results revealed that **2** had reasonable IC_{50} and the highest activity, while **1** displayed less cytotoxic activity. Additional mechanistic investigation revealed that **2** induced significant cancer cell death by apoptosis.

4 | EXPERIMENTAL

4.1 | General procedures and materials

All reactions were carried out under an argon atmosphere using standard Schlenk techniques. NMR (^{1}H and ^{13}C{^{1}H}) spectra were recorded with a Bruker Avance DPX 400 MHz instrument and are referenced to the residual peak of the solvent, i.e. DMSO-d_6 or $CDCl_3$ (^{1}H and ^{13}C). The chemical shifts were measured in ppm and coupling constants in Hz. ^{13}C{^{1}H} NMR assignment was achieved via DEPT 135. The melting point values were measured using a Buchi 510. Microanalyses were performed using a Vario EL CHNS elemental analyser. Fourier transform IR spectroscopy with KBr pellets was performed using a Bruker Vector 22 FT-IR instrument. Benzyl isocyanide ($PhCH_2NC$) and pyrimidine-2-thiol (HSpyN) were purchased from Acros and Aldrich, respectively. Also, all solvents were purchased from Aldrich and used without further purification. Complex **A** was prepared as reported in the literature. [37] The chemical shift assignments are based on the NMR labelling for the ligands as shown in Figures S1 and S2.

4.2 | Potassium Pyrimidine-2-thiolate (KSpyN)

To a solution of KOH (125 mg, 2.23 mmol) in MeOH (5 ml), a solution of HSpyN (250 mg, 2.23 mmol) in MeOH (10 ml) was added. The resulting yellow solution was stirred at room temperature for 1 h, and then the solvent was evaporated to dryness. The residue was treated with ^{i}PrOH (2 ml), and the resulting yellow solid was filtered and dried. Yield: 305 mg (91%). Anal. Calcd for $C_4H_3KN_2S$ (150.24) (%): C, 31.98; H, 2.01; N, 18.65. Found (%): C, 31.91; H, 2.03; N, 18.61%. ^{1}H NMR (DMSO-d_6, δ, ppm): 6.43 (t, $^3J_{HH}$ = 4.7 Hz, 1H, H^i), 7.94 (d, $^3J_{HH}$ = 4.7 Hz, 2H, H^h). ^{13}C{^{1}H} NMR (δ, ppm): 110.8 (s, C^i), 155.2 (s, 2C, C^h), 188.4 (s, C^g).

4.3 | [(PhCH$_2$NC)AuCl] (1)[13,38]

To a solution of **A** (200 mg, 0.68 mmol) in CH_2Cl_2 (20 ml), 1 eq. of $PhCH_2NC$ (83 μl, 0.68 mmol) was added. The mixture was stirred at room temperature for 1 h and then the solvent was concentrated to a small volume (*ca* 1 ml) under vacuum, and *n*-pentane (5 ml) was added to give **1** as a white solid, which was filtered and washed with *n*-pentane (2 × 3 ml) and dried. Yield: 197 mg (83%); m.p. 138 °C. Anal. Calcd for C_8H_7AuClN (349.57) (%): C, 27.49; H, 2.02; N, 4.01. Found (%): C, 27.61; H, 2.05; N, 4.06. IR (KBr, cm^{-1}): 2260 (s, $\nu_{C\equiv N}$). ^{1}H NMR ($CDCl_3$, δ, ppm): 4.87 (s, 2H, H^e), 7.35 (dd, $^3J_{HH}$ = 7.7 Hz, $^4J_{HH}$ = 1.4 Hz, 2H, H^a), 7.46–7.43 (m, 3H, H^b and H^c). ^{13}C{H} NMR (δ, ppm): 48.2 (t, $^1J_{CN}$ = 7 Hz, C^e), 127.5 (s, 2C, C^a), 129.4 (s, C^d), 129.6 (s, 2C, C^b), 129.7 (s, C^c), 135.6 (t, $^1J_{CN}$ = 26 Hz, C^f).

4.4 | [(PhCH$_2$NC)au(η^1-S-spy)] (2)

An equimolar amount of KSpyN (43 mg, 0.29 mmol) was dissolved in MeOH–acetone (2:8 ml) and added to a solution of **1** (100 mg, 0.29 mmol) in CH_2Cl_2 (15 ml). The reaction mixture was stirred at room temperature for 15 h. Then, solvent was removed under reduced pressure and the residue was extracted with CH_2Cl_2 (10 ml). The obtained colourless solution was filtered through celite and the filtrate was concentrated to a small volume (*ca* 1 ml) under vacuum, and *n*-pentane (5 ml) was added to give **2** as a white solid, which was filtered and washed with *n*-pentane (3 × 3 ml) and dried. Yield: 86 mg (71%); m.p. 125 °C. Anal. Calcd for $C_{12}H_{10}AuN_3S$ (425.26) (%): C, 33.89; H, 2.37; N, 9.88. Found (%): C, 33.97; H, 2.41; N, 9.91. IR (KBr, cm^{-1}): 2247 (s, $\nu_{C\equiv N}$). ^{1}H NMR ($CDCl_3$, δ, ppm): 4.84 (s, 2H, H^e), 6.82 (t, $^3J_{HH}$ = 4.9 Hz, 1H, H^i), 7.36 (dd, $^3J_{HH}$ = 7.5 Hz, $^4J_{HH}$ = 1.7 Hz, 2H, H^a), 7.45–7.42 (m, 3H, H^b and H^c), 8.34 (d, $^3J_{HH}$ = 4.9 Hz, 2H, H^h). ^{13}C{^{1}H} NMR (δ, ppm): 48.0 (t, $^1J_{CN}$ = 7 Hz, C^e), 115.8 (s, C^i), 127.5 (s, 2C, C^a), 129.4 (s, C^d), 129.6 (s, 2C, C^b), 129.7 (s, C^c), 146.2 (t, $^1J_{CN}$ = 23 Hz, C^f), 156.8 (s, 2C, C^h), 179.6 (s, C^g).

4.5 | Crystal structure determination and refinement

X-ray diffraction measurements were carried out using a STOE IPDS 2 T diffractometer with graphite-monochromated Mo Kα radiation. A single crystal suitable for X-ray analysis was obtained from CH_2Cl_2–*n*-hexane solution (at room temperature) and mounted on a glass fibre and used for data collection. Cell constants and an orientation matrix for data collection were obtained by least-square refinement of the diffraction data for **1**. Diffraction data were collected in a series of ω scans in 1° oscillations and integrated using the STOE X-AREA software package.[45] Numerical absorption correction was applied using X-Red32 software. The structure was solved by direct methods and subsequent difference Fourier maps and then refined on F^2 by a full-matrix least-squares procedure using anisotropic displacement parameters. Atomic

factors are from the International Tables for X-ray Crystallography. All non-hydrogen atoms were refined with anisotropic displacement parameters. Hydrogen atoms were placed in ideal positions and refined as riding atoms with relative isotropic displacement parameters. All refinements were performed using the X-STEP32, SHELXL-2014 and WinGX-2013.3 programs.[46–50] CCDC-1571094 (for **1**) contains the supplementary crystallographic data for this paper. This data can be obtained free of charge from the Cambridge Crystallographic Data Centre via www.ccdc.cam.ac.uk/data_request/cif.

4.6 | Biological assay

4.6.1 | Cell lines and cell culture

Human cancer cell lines MCF-7, SKOV3 and A549 were purchased from National Cell Bank of Iran (NCBI, Pasteur Institute, Tehran, Iran). All cells were cultured in Dulbecco's modified Eagle medium (Biosera, UK), except MCF-7 cells which were cultured in RPMI 1640 (Sigma Aldrich), supplemented with 10% foetal bovine serum (Gibco, UK) and 1% penicillin–streptomycin and were incubated at 37 °C in a humidified CO_2 incubator.

4.6.2 | MTT assay

Standard 3-(4,5-dimethylthiazol-yl)-2,5-diphenyltetrazolium bromide (MTT) assay was used for assessing cytotoxic activities of **1** and **2** according to a known protocol.[3,51,52] The cells were harvested and plated in 96-well microplates at a density of 1×10^4 cells per well in 100 μl of complete culture medium. After 24 h of incubation, the cells were treated with five different concentrations of the Au complexes ranging from 1 to 100 μM in a triplicate manner. Each compound was dissolved in DMSO. To avoid bystander cytotoxic effect, the final concentration of DMSO was maintained at about 0.1%. Following 48 h of incubation at 37 °C in a humidified CO_2 incubator, media were completely removed and replaced with 100 μl of new media containing 0.5 mg ml^{-1} MTT solution and the plate were incubated for 3 h at room temperature. The media containing MTT were then discarded, and 150 μl of DMSO was added to each well to dissolve the formazan crystals. The plates were then incubated for 30 min at 37 °C in the dark. The absorbance of individual wells was read at 492 nm using a microplate ELISA reader. The data were analysed using Excel 2013 and CurveExpert 1.4 and the 50% inhibitory concentration (IC_{50}) of each compound was determined. Each experiment was conducted three times for each complex in a triplicate manner. Data are presented as mean ± standard deviation (SD).

4.6.3 | Apoptosis determination

MCF-7 cells at 0.5×10^5 cells per millilitre of complete culture medium were seeded in a 24-well culture plate. Following 24 h incubation, the cells were treated with different concentrations of **2** (2.5, 5 and 10 μM). Untreated samples with equivalent DMSO concentration were used as the controls. The cells were then incubated at 37 °C with 5% CO_2 for 48 h. Treated and untreated cells were then harvested and washed twice with cold cell staining buffer (BioLegend). An amount of 50 μl of cells re-suspended in Annexin V binding buffer was then added to polystyrene round-bottom tubes (BD Bioscience, USA). Amounts of 2 μl of FITC-conjugated Annexin V and 2 μl of 7-AAD solution were added to the cells and vortexed gently and incubated for 15 min at room temperature in the dark. An amount of 300 μl of Annexin V binding buffer was added to each tube and analysed immediately using a four-colour FACSCalibur flow cytometer (BD Bioscience, USA) with appropriate setting. The data were analysed using flowJo software packages.

ACKNOWLEDGEMENTS

M. H. B. gratefully acknowledges the financial support through the startup funds from the University of Arkansas. The Institute for Advanced Studies in Basic Sciences (IASBS) Research Council, and Medicinal Chemistry, School of Pharmacy, Ahvaz Jundishapur University of Medical Sciences (B-9557, B-9637) are also gratefully acknowledged.

ORCID

Masood Fereidoonnezhad http://orcid.org/0000-0003-3405-0228
Hamid R. Shahsavari http://orcid.org/0000-0002-2579-2185
M. Hassan Beyzavi http://orcid.org/0000-0002-6415-8996

REFERENCES

[1] B. Rosenberg, L. VanCamp, J. E. Trosko, V. H. Mansour, *Nature* **1969**, *222*, 385.

[2] E. Guerrero, S. Miranda, S. Lüttenberg, N. Fröhlich, J.-M. Koenen, F. Mohr, E. Cerrada, M. Laguna, A. Mendía, *Inorg. Chem.* **2013**, *52*, 6635.

[3] M. Fereidoonnezhad, M. Niazi, Z. Ahmadipour, T. Mirzaee, Z. Faghih, Z. Faghih, H. R. Shahsavari, *Eur. J. Inorg. Chem.* **2017**, *2247*.

[4] C. Nardon, G. Boscutti, D. Fregona, *Anticancer Res.* **2014**, *34*, 487.

[5] H. G. Raubenheimer, H. Schmidbaur, *J. Chem. Educ.* **2014**, *91*, 2024.

[6] M. D. Đurović, Ž. D. Bugarčić, R. van Eldik, *Coord. Chem. Rev.* **2017**, *338*, 186.

[7] G. J. Hutchings, M. Brust, H. Schmidbaur, *Chem. Soc. Rev.* **2008**, *37*, 1759.

[8] F. Mohr, *Gold Chemistry: Applications and Future Directions in the Life Sciences*, 2nd ed., Wiley-VCH, Weinheim **2009**.

[9] A. Laguna, *Modern Supramolecular Gold Chemistry: Gold-Metal Interactions and Applications*, Wiley-VCH, Weinheim **2008**.

[10] H. Schmidbaur, *Chem. Soc. Rev.* **1995**, *24*, 391.

[11] M. A. Malwitz, S. H. Lim, R. L. White-Morris, D. M. Pham, M. M. Olmstead, A. L. Balch, *J. Am. Chem. Soc.* **2012**, *134*, 10885.

[12] W. Schneider, K. Angermaier, A. Sladek, H. Schmidbaur, *Z. Naturforsch. B* **1996**, *51*, 790.

[13] R. Manzano, F. Rominger, A. S. K. Hashmi, *Organometallics* **2013**, *32*, 2199.

[14] A. Collado, A. Gomez-Suarez, A. R. Martin, A. M. Z. Slawin, S. P. Nolan, *Chem. Commun.* **2013**, *49*, 5541.

[15] Z. Han, J. I. Bates, D. Strehl, B. O. Patrick, D. P. Gates, *Inorg. Chem.* **2016**, *55*, 5071.

[16] T. Seki, K. Sakurada, M. Muromoto, S. Seki, H. Ito, *Chem. – Eur. J.* **2016**, *22*, 1968.

[17] A. Johnson, M. C. Gimeno, *Chem. Commun.* **2016**, *52*, 9664.

[18] I. Ott, *Coord. Chem. Rev.* **2009**, *253*, 1670.

[19] L. Joao Carlos, R. Laura, *Anti-Cancer Agents Med. Chem.* **2011**, *11*, 921.

[20] E. García-Moreno, S. Gascón, E. Atrián-Blasco, M. J. Rodriguez-Yoldi, E. Cerrada, M. Laguna, *Eur. J. Med. Chem.* **2014**, *79*, 164.

[21] L. Hao, M. A. Mansour, R. J. Lachicotte, H. J. Gysling, R. Eisenberg, *Inorg. Chem.* **2000**, *39*, 5520.

[22] J. A. Robson, F. Gonzàlez de Rivera, K. A. Jantan, M. N. Wenzel, A. J. P. White, O. Rossell, J. D. E. T. Wilton-Ely, *Inorg. Chem.* **2016**, *55*, 12982.

[23] T. Zou, C. T. Lum, C.-N. Lok, J.-J. Zhang, C.-M. Che, *Chem. Soc. Rev.* **2015**, *44*, 8786.

[24] E. Atrián-Blasco, S. Gascón, M. J. Rodríguez-Yoldi, M. Laguna, E. Cerrada, *Inorg. Chem.* **2017**, *56*, 8562.

[25] M. Dadkhah Aseman, S. M. Nabavizadeh, H. R. Shahsavari, M. Rashidi, *RSC Adv.* **2015**, *5*, 22692.

[26] M. Niazi, H. R. Shahsavari, M. Golbon Haghighi, M. R. Halvagar, S. Hatami, B. Notash, *RSC Adv.* **2016**, *6*, 95073.

[27] E. S. Raper, *Coord. Chem. Rev.* **1996**, *153*, 199.

[28] P. Römbke, A. Schier, F. Wiesbrock, H. Schmidbaur, *Inorg. Chim. Acta* **2003**, *347*, 123.

[29] A. Gutierrez, C. Cativiela, A. Laguna, M. C. Gimeno, *Dalton Trans.* **2016**, *45*, 13483.

[30] Y. Hokai, B. Jurkowicz, J. Fernández-Gallardo, N. Zakirkhodjaev, M. Sanaú, T. R. Muth, M. Contel, *J. Inorg. Biochem.* **2014**, *138*, 81.

[31] O. Dada, D. Curran, C. O'Beirne, H. Müller-Bunz, X. Zhu, M. Tacke, *J. Organometal. Chem.* **2017**, *840*, 30.

[32] E. Y. Chia, S. Naeem, L. Delaude, A. J. P. White, J. D. E. T. Wilton-Ely, *Dalton Trans.* **2011**, *40*, 6645.

[33] Y. F. Mui, J. Fernández-Gallardo, B. T. Elie, A. Gubran, I. Maluenda, M. Sanaú, O. Navarro, M. A. Contel, *Organometallics* **2016**, *35*, 1218.

[34] V. P. Dyadchenko, N. M. Belov, D. A. Lemenovskii, M. Y. Antipin, K. A. Lyssenko, A. E. Bruce, M. R. M. Bruce, *J. Organometal. Chem.* **2010**, *695*, 304.

[35] W. Schneider, A. Bauer, H. Schmidbaur, *Organometallics* **1996**, *15*, 5445.

[36] V. P. Dyadchenko, N. M. Belov, M. A. Dyadchenko, Y. L. Slovokhotov, A. M. Banaru, D. A. Lemenovskii, *Russ. Chem. Bull. Int. Ed.* **2010**, *59*, 539.

[37] M.-C. Brandys, M. C. Jennings, R. J. Puddephatt, *J. Chem. Soc. Dalton Trans.* **2000**, *4601*.

[38] A. S. K. Hashmi, T. Hengst, C. Lothschütz, F. Rominger, *Adv. Synth. Catal.* **2010**, *352*, 1315.

[39] J. Zakrzewski, B. Huras, A. Kiełczewska, *Synthesis* **2016**, *48*, 85.

[40] K. Hojoh, H. Ohmiya, M. Sawamura, *J. Am. Chem. Soc.* **2017**, *139*, 2184.

[41] S. Martínez-Salvador, L. R. Falvello, A. Martín, B. Menjón, *Chem. – Eur. J.* **2013**, *19*, 14540.

[42] A. Meyer, A. Gutiérrez, I. Ott, L. Rodríguez, *Inorg. Chim. Acta* **2013**, *398*, 72.

[43] P. Hikisz, Ł. Szczupak, A. Koceva-Chyła, L. Oehninger, I. Ott, B. Therrien, J. Solecka, K. Kowalski, *Molecules* **2015**, *20*, 19699.

[44] A. A. Seliman, M. Altaf, A. T. Onawole, S. Ahmad, M. Y. Ahmed, A. A. Al-Saadi, S. Altuwaijri, G. Bhatia, J. Singh, A. A. Isab, *J. Organometal. Chem.* **2017**, *848*, 175.

[45] *X-AREA: program for the acquisition and analysis of data, Version 1.30*, Stoe & Cie GmbH, Darmstadt, Germany **2005**.

[46] M. N. Burnett, C. K. Johnson, *ORTEP-III Report ORNL-6895*, Oak Ridge National Laboratory, Oak Ridge, TN **1996**.

[47] P. Coppens, L. Leiserowitz, D. Rabinovich, *Acta Crystallogr.* **1965**, *18*, 1035.

[48] L. J. Farrugia, *J. Appl. Crystallogr.* **1999**, *32*, 837.

[49] C. F. Macrae, P. R. Edgington, P. McCabe, E. Pidcock, G. P. Shields, R. Taylor, M. Towler, J. van der Streek, *J. Appl. Crystallogr.* **2006**, *39*, 453.

[50] G. M. Sheldrick, *Acta Crystallogr. A* **2008**, *64*, 112.

[51] M. Fereidoonnezhad, B. Kaboudin, T. Mirzaee, R. Babadi Aghakhanpour, M. Golbon Haghighi, Z. Faghih, Z. Faghih, Z. Ahmadipour, B. Notash, H. R. Shahsavari, *Organometallics* **2017**, *36*, 1707.

[52] M. Fereidoonnezhad, M. Niazi, M. Shahmohammadi Beni, S. Mohammadi, Z. Faghih, Z. Faghih, H. R. Shahsavari, *ChemMedChem* **2017**, *12*, 456.

SUPPORTING INFORMATION

Additional Supporting Information may be found online in the supporting information tab for this article.

How to cite this article: Fereidoonnezhad M, Shahsavari HR, Lotfi E, et al. (Benzyl isocyanide) gold(I) pyrimidine-2-thiolate complex: Synthesis and biological activity. *Appl Organometal Chem*. 2018;e4200. https://doi.org/10.1002/aoc.4200